Predator–Prey Molecular Ecosystems

Teruo Fujii and Yannick Rondelez*

LIMMS/CNRS-IIS, Institute of Industrial Science, The University of Tokyo, 4-6-1 Komaba, Meguro-ku, Tokyo 153-8505, Japan

ABSTRACT Biological organisms use intricate networks of chemical reactions to control molecular processes and spatiotemporal organization. In turn, these living systems are embedded in self-organized structures of larger scales, for example, ecosystems. Synthetic *in vitro* efforts have reproduced the architectures and behaviors of simple cellular circuits. However, because all these systems share the same dynamic foundations, a generalized molecular programming strategy should also support complex collective behaviors, as seen, for example, in animal populations. We report here the bottom-up assembly of chemical systems that reproduce *in vitro* the specific dynamics of ecological communities. We experimentally observed unprecedented molecular behaviors, including predator–prey oscillations, competition-induced chaos, and symbiotic synchronization. These synthetic systems are tailored through a novel, compact, and versatile design strategy, leveraging the programmability of DNA interactions under the precise control of enzymatic catalysis. Such self-organizing assemblies will foster a better appreciation of the molecular origins of biological complexity and may also serve to orchestrate complex collective operations of molecular agents in technological applications.

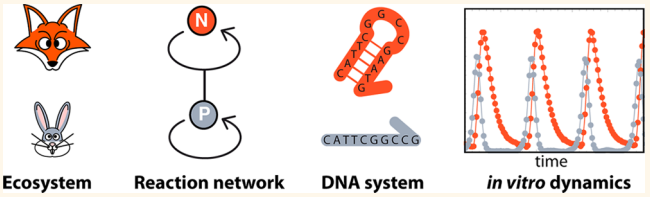

KEYWORDS: reaction networks · molecular programming · DNA nanotechnology · predator–prey · oscillations · dynamic systems

The classic Lotka predator–prey (PP) equations[1,2] are famous for predicting the counterintuitive fact that sustained oscillations are a natural mode of population coexistence in ecological food chains. Modern mathematical models of ecosystems incorporate additional interactions such as competition or symbiosis and predict a rich array of behaviors including, along with stable coexistence, oscillations and chaos. They apply to a variety of agent-based communities, from ecology[3−6] to economics.[7,8] Surprisingly, molecular systems seem to depart from this ubiquity, as there is no reported implementation of the PP paradigm in the chemical world.[9] The possibility of biochemical analogues of ecological dynamics was foreseen some years ago,[10] with the description of a molecular mechanism for prey growth and predation based on two interdependent DNA–RNA amplification cycles. The authors experimentally demonstrated the coupling between the two molecular species, but experimental oscillations could not be observed[11] and would have moreover required an open reactor to occur. More recently, the theoretical construction of an oscillating chemical PP system was used as a demonstration of the potential versatility of DNA reaction networks.[12]

Nonetheless, Lotka's initial insight about PP oscillations was based on chemical kinetics;[1,13] hypotheses concerning prebiotic molecular "worlds" also suggest a role for PP dynamics,[14,15] and the ubiquity of the predatory rule among living systems strongly advocates for a chemical root to the phenomenon. Besides, compliant and fast *in vitro* PP systems would represent an unmatched opportunity to study experimentally the infinite variety of dynamics predicted to emerge from trophic interactions.

Theoretically, DNA-based molecular programs offer a platform for the design of dynamic reaction networks with arbitrary topologies,[12] but practical examples are more restricted, for example, to models of simple cellular circuits.[16−20] Here we present an effective experimental approach for the design of out-of-equilibrium *in vitro* behaviors, and we apply it to the design of the elusive predator–prey chemical ecosystem. We start with the core two-species system and analyze its robust oscillatory signature. We then rationally assemble a variety of molecular ecosystems with a higher number of species and interactions. All of them correspond to ecologically important, but chemically novel, mechanisms and dynamics.

RESULTS AND DISCUSSION

Building a PP Biochemical Oscillator. PP systems recapitulate three phenomena: prey

* Address correspondence to rondelez@iis.u-tokyo.ac.jp.

Received for review September 20, 2012 and accepted November 23, 2012.

Published online 10.1021/nn3043572

Published online November 23, 2012 10.1021/nn3043572

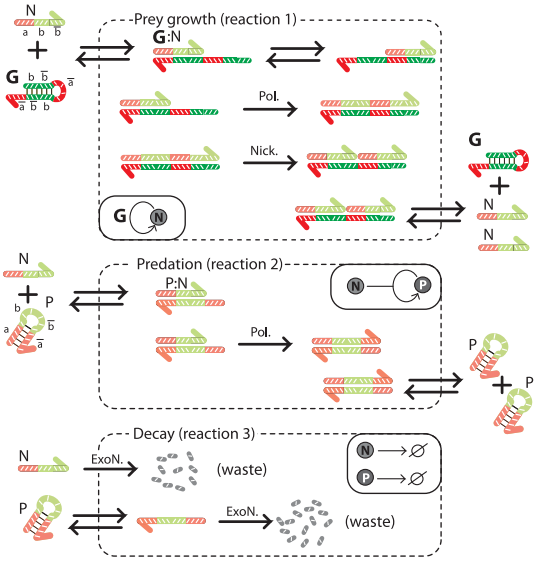

Figure 1. General design of the predator–prey reaction network. The global reactions 1–3 are constructed from DNA polymerization–depolymerization reactions in order to implement the correct formal relations between the molecular species. The template G (in strong colors) is the only stable sequence in the system. Other oligonucleotides (predator P and prey N, in light colors) are dynamically produced and degraded in the presence of a polymerase (Pol.), a nicking enzyme (Nick.), and an exonuclease (ExoN.). Sequence domains are color-coded. Hashes emphasize the buildup of the palindromic structure of the predator.

growth (autocatalytic reaction 1), predation (autocatalytic reaction with consumption or prey, reaction 2), and decay (reaction 3).

$$N \rightarrow 2N \quad (1)$$

$$N + P \rightarrow 2P \quad (2)$$

$$N, P \rightarrow \varnothing \quad (3)$$

Figure 1 shows how the corresponding chemical reactions can be compiled using DNA biochemistry. The construction starts with the predation reaction 2, which is the defining feature of PP systems. This reaction describes the growth of the predators through the consumption of prey and refers to a replicator with exponential dynamics.[21] Since our goal is to integrate this step in larger networks of reactions, we also require a generic design, which may support many instantiations. We initially noticed that, formally, reaction 2 may stand for the DNA polymerase-catalyzed elongation of a primer on a template, provided three conditions. (i) The predator P must have a palindromic sequence, so that the elongation of a primer using P as a template will produce a second copy of P (in other words, there must be a center of symmetry in the middle of the P−P duplex).[22] (ii) The prey N should be long enough to prime the polymerase. (iii) P should be short enough to significantly dissociate into monomeric species at the experimental temperature (this last condition serves to avoid product inhibition). Under appropriate conditions and temperature, we found that these design constraints can be met by a number of sequences. We selected one of these sequences as the basis of a first PP system, named PP_1 and comprising the prey N_1, the predator P_1, and the template G_1 (Figure 2a). Figure 2b shows the exponential growth of the short 14 base palindromic P_1 when feeding on 10 base N_1 as primers. This reaction is observed here through the increase of a green fluorescence signal produced by a DNA-intercalating dye: predators produce more fluorescence than prey, so the total signal increases sigmoidally until all prey are converted into predators (see Supporting Information Figure S9 for additional plots and curve fitting).

We now turn to reaction 1, where the prey N triggers its own generation in a simple loop. In DNA biochemistry, this may translate into an isothermal amplification scheme based on repetitive enzymatic extensions and nicking on a dual-repeat DNA template.[16] The only sequence constraint at this stage is the presence of a recognition site at the appropriate position in the sequence of the prey. In Figure 2c, we use a template (called G_1) designed to amplify the prey N_1, that is, the one used by the predator P_1 to fuel its replication. In isolation (in the absence of predator), the autocatalytic prey amplification reaction generates an exponential increase of the prey, again observed through an increase in the green fluorescence signal.

Reaction 3 implies that all of the species have a limited lifetime in the system. From a dynamic, or thermodynamic, point of view, this step is essential to avoid a runaway of the system and to allow the existence of bounded attractors, yielding, for example, stable periodic trajectories. In a closed setting, this sink function needs to be provided internally. Here we use a thermophilic exonuclease,[23] able to digest both P_1 and N_1 into inactive monomers (Figure 2d). The global energy flux for reactions 1−3 will then start from activated, but metastable, nucleotides (dNTPs), which are catalytically incorporated in short oligonucleotides and subsequently depolymerized into inactivated (waste) monomers (dNMPs). The batch design used here implies a finite lifetime for the system, limited at the very least by the exhaustion of dNTPs.

In Figure 2e, predation and degradation reactions are assembled, resulting in a spiking behavior: if a sufficient amount of prey is initially present, the predator population starts to grow, but the limited lifetime of each species ultimately brings the system back to zero. Finally, when reactions 1, 2, and 3 are combined, the prey population is able to recover after the predator decay, and this isothermal system produces repetitive spikes of both species (Figure 2f). When conditions are adequately tuned by selecting enzymes, temperature, and G_1 concentration, one observes sustained oscillations, a landmark property of PP systems. These oscillations have a period of one to

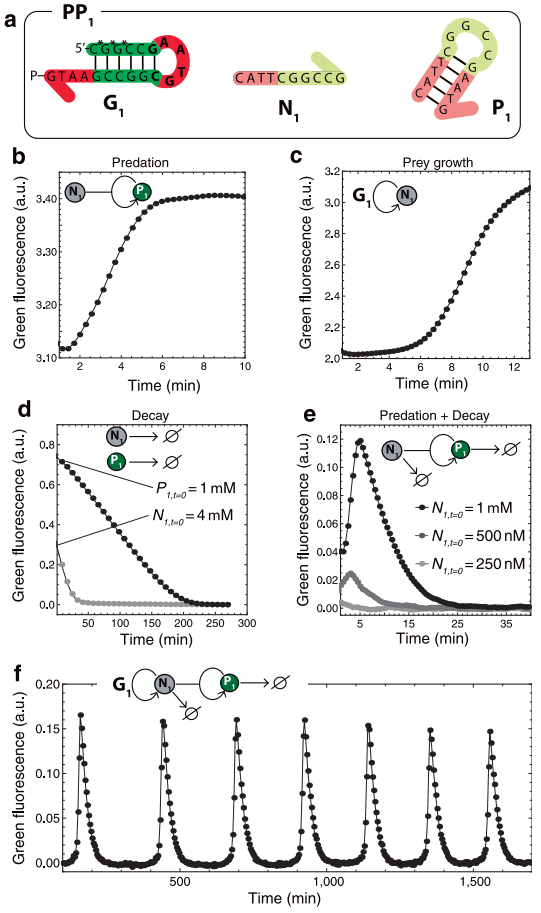

Figure 2. Assembly and monitoring of the predator−prey system PP_1 (isothermal batch experiments at 46.5 °C). The green fluorescent signal observed in all of the plots is produced by an intercalating dye that does not resolve prey and predators. (a) Sequences of the 20 base long dual repeat G_1 template, the 10 base prey N_1, and the 14 base predator P_1. G_1 has the Nb.BsmI recognition site in bold, phosphorothioate backbone modifications—used to protect it from ttRecJ—indicated by *, and a phosphate modification on the 3′ end to block spurious extension by the polymerase. (b) Predation (reaction 2) involves the duplication of palindromic predators, using—and consuming—shorter prey (initially 100 nM) as primers. The resulting duplex dissociates into monomeric species, creating an autocatalytic feedback. The reaction, driven by the polymerase only, was seeded with a small concentration of P_1. (c) Prey amplification (reaction 1) *via* templated DNA duplication requires the presence of G_1 (here at 200 nM), *Bst* polymerase large fragment, and the nicking enzyme Nb.BsmI. The reaction is initiated with a small amount of N_1. The leveling-off after 10 min is due to the saturation of the fluorescence, mostly produced by the template in double-stranded (prey bound) form (see Supporting Information section 3 and Figure S10 for details). (d) Degradation (reaction 3) is catalyzed by an exonuclease. Both N_1 and P_1 are digested by ttRecJ (here at 8 nM), albeit with different maximum rates and affinities. (e) Combining predation and decay produces a pulse of predators at the condition that $N_{1,t=0}$ is large enough ($P_{1,t=0}$ = 1 nM in all three experiments shown). (f) In the presence of template G_1 (160 nM) and the three enzymes, the prey amplification mechanism resumes after the predator population has shrunk, and sustained oscillations are obtained.

a few hours and may last for days, until enzymes are gradually inactivated or dNTPs depleted.

Because genetic information is passed from one strand to the next in each polymerization step, the genetic information encoding the full reaction network is contained in the sole sequence of the template or equivalently in that of the prey N_1 (CATTCGGCCG). The dynamic operation of this system is permitted by a set of three thermophilic enzymes, a DNA polymerase (*Bst* large fragment), and nicking enzyme (Nb.BsmI) and an exonuclease (ttRecJ[23]).

Multiplexed Monitoring. A complete characterization of the dynamics requires the independent monitoring of both prey and predator concentrations. To do so, a yellow fluorescent dye is attached to the 3′ end of the template G_1. The fluorescence intensity of this dye will depend on the single-stranded or double-stranded status of its end of the G_1 template[24] and will therefore yield a signal dominated by the prey contribution (Figure 3a). From the deconvolution of the green and yellow fluorescent channels, we now obtain two traces, revealing a clear phase shift between the oscillations of the two species (Figure 3b,c; see Supporting Information for details). As expected, the prey population comes first, disappears during the predator burst, and resumes its growth when predators come back to a low level. The time plots are of sufficient quality to be converted in 2D fluorescence trajectories (Figure 3d,e). These plots suggest the convergence toward a limit cycle (necessarily transient in this closed system) for intermediate template concentrations. Pseudo-limit-cycle oscillations are further supported by experiments initiated with different initial conditions $N_{1,t=0}$ and $P_{1,t=0}$, which converge toward the same stable orbit (Supporting Information Figure S2).

Mathematical Model. Reactions 1 and 2 are composite chemical processes which, under simplifying assumptions, can be reduced to simple kinetic descriptions (Supporting Information section 2 and Figures S3−S6). Reaction 3 is an enzymatic transformation of the Michaelis−Menten type. We thus derive a simple—but importantly still mechanistic—two-variable model belonging to the family of PP equations. It can be reduced to a non-dimensional form with five parameters:

$$\frac{dn}{dt} = \frac{g \cdot n}{1 + \beta \cdot g \cdot n} - p \cdot n - \lambda \cdot \delta \frac{n}{1 + p}$$

$$\frac{dp}{dt} = p \cdot n - \delta \frac{p}{1 + p}$$

where n, p, and g are the scaled total concentrations of prey, predator, and template, β is a saturation term, and δ and $\lambda \cdot \delta$ are the scaled first-order decay rates for predator and prey, respectively.

A first set of parameter values can be estimated from the kinetic analysis of isolated reactions 1−3 (Supporting Information section 3 and Figures S7−S10). Injected in the model, this raw parameter set yields the following numerical predictions (Supporting Information Figure S11): as the total concentration of G_1 increases, the initial stable

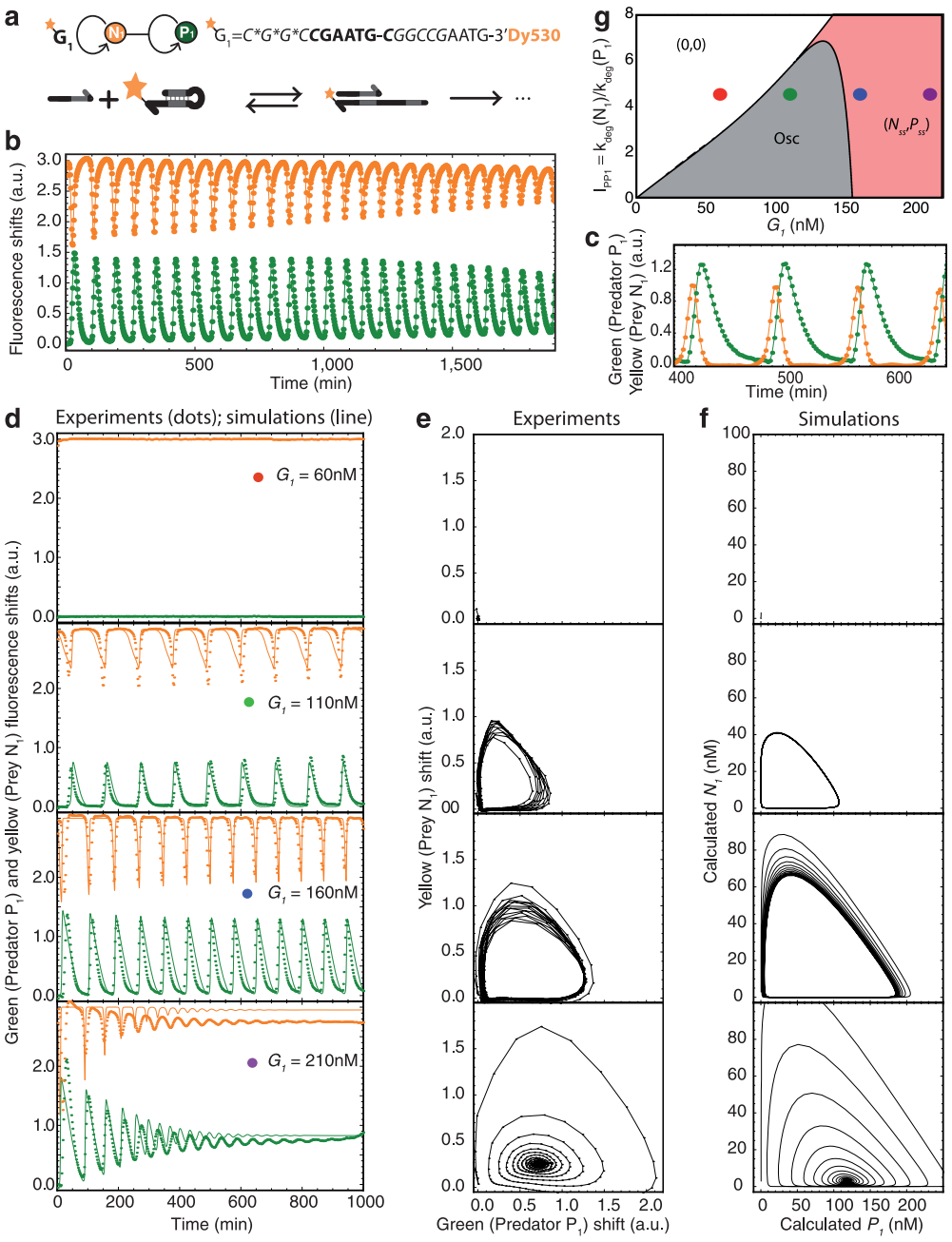

Figure 3. Two-color experimental PP system and two-species mathematical model. (a) N quenching[24] allows the real-time monitoring of the prey population: upon hybridization of prey on the 3′ end of template G_1, the yellow fluorescent modification is reversibly quenched. (b) Time course of green and yellow fluorescent signals (offset for clarity). The yellow signal reports mostly on the amount of prey N_1 in the system, while the green signal is dominated by the predator P_1. (c) After deconvolution, one observes a clear phase delay between the oscillations of the two species. Note that fluorescence is given in arbitrary units. (d) Experimental and simulated time plots for various G_1 concentrations. Dots show the deconvoluted prey (yellow) and predator (green) fluorescent contributions. The continuous line is the model prediction, using the same set of optimized parameters for all four experiments. Stable oscillations are observed for a given range of G_1 concentrations, above which they get damped, and below which flat responses are seen. (e) Experimental 2D trajectories in the fluorescence space. (f) Computed trajectories in the P_1–N_1 phase space. (g) Stable coexistence (N_{ss}, P_{ss}), extinction (0,0), and oscillatory (Osc) regions of the two-variable model with optimized parameters (see Supporting Information Figures S3–S6 for details). Colored disks indicate the parameter values corresponding to the plots in d, e, and g.

state of complete extinction (no species) gives place to a permanently oscillating ecosystem of prey and predators. From this point on, oscillations persist until G_1 is approximately doubled, after which they get damped and converge toward a stable steady state where both species coexist. These predictions are in line with the experimental observations (Figure 3d,e). Moreover, after slightly refining the parameters, an almost quantitative agreement between model and data can be obtained for all sampled G_1 concentrations (Figure 3d–f and Supporting Information Table S5). This is remarkable given the simplicity of this two-variable model.

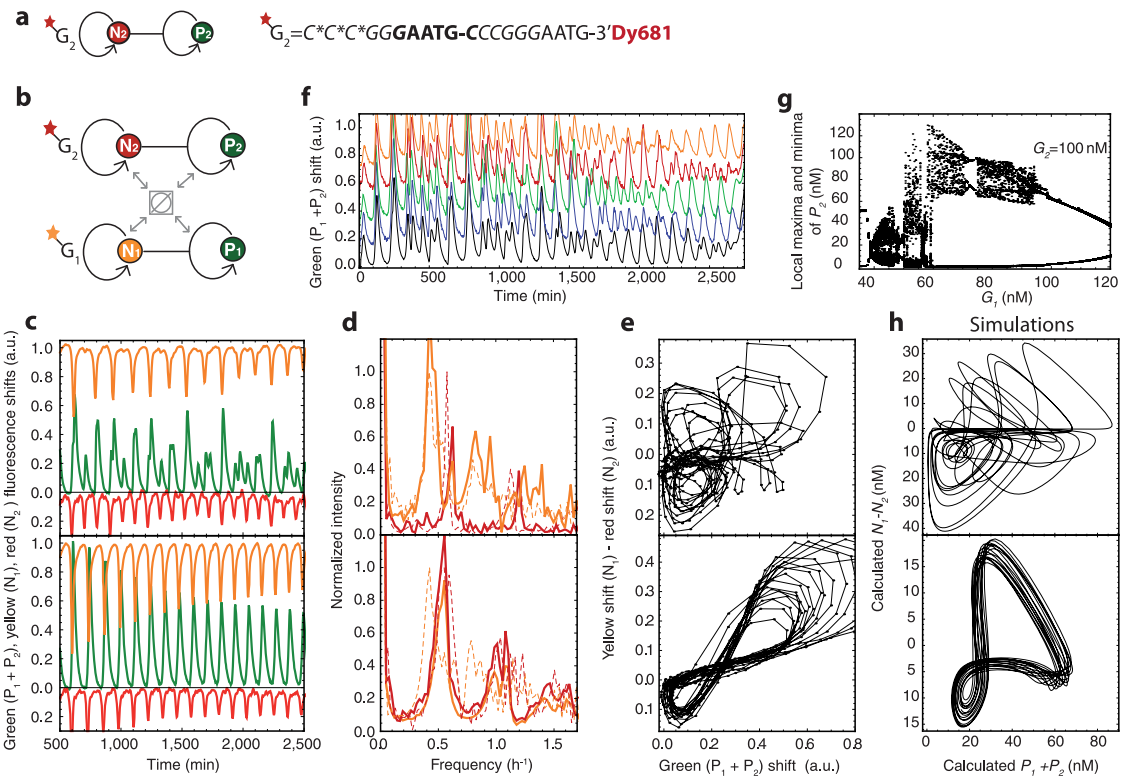

Figure 4. Two predator–prey pairs competing for enzymatic resources. (a) PP_2 system and its fluorescent template G_2. (b) Schematic of the network comprising four species competing for the enzymes (collectively represented as a gray box). (c) Time plots of fluorescent records in the yellow, red, and green channels, corresponding, respectively, to N_1, N_2, and, after subtraction of the preys' green contributions, $P_1 + P_2$. Yellow and red traces are offset for clarity (top: an experiment with G_1 = 50 nM and G_2 = 100 nM; bottom: an experiment with G_1 = 60 nM and G_2 = 110 nM; also shown as Supporting Information movies S1 and S2; see Supporting Information section 5 and Figures S14–S18 for additional experiments). Alternation of long and short periods can be distinguished in the yellow trace of the top experiment. (d) Discrete Fourier transform of the yellow and red signals are displayed in the corresponding color (thick lines) and compared to the situation where each pair is present alone in solution (dashed lines), with the same template concentration. (e) Same data are plotted as N_1–N_2 *versus* P_1+P_2, in order to be visualized in 2D. (f) Reaction as in c (top graph) is started with slightly different initial conditions (black: N_1, N_2, P_1, P_2 = 10 nM; blue, green, red, orange: same as black plus, respectively, 2 nM of N_1, N_2, P_1, or P_2 to produce the initial difference). The divergence of the trajectories in 3D fluorescent space is shown as Supporting Information movie S3. (g) Simulated bifurcation plot showing all local maxima and minima over 5000 min of the P_2 trajectory for G_2 = 100 nM and varying concentrations of G_1. (h) Simulated trajectories shown as N_1–N_2 *versus* P_1+P_2 (top, G_1 = 55 nM, G_2 = 100 nM; bottom, G_1 = 60 nM, G_2 = 110 nM).

Multispecies Systems. Besides PP interactions, the behavior of real ecosystems is also controlled by other types of interactions and primarily by the competition for resources.[3] Such additional couplings are capable of producing intricate dynamics and especially chaos in multispecies systems.[6,25] To study experimentally the consequences of competition in a molecular ecosystem, we have built a second predator−prey pair, PP_2, based on the prey N_2 (CATTCCCGGG), the predator P_2, and the template G_2. N_2 is four mutations away from N_1, and given the short length of the DNA species used here, this insures orthogonality between the two PP pairs in terms of binding constants (see Supporting Information Table S2). In the same experimental conditions as before (*i.e.*, temperature, buffer, and enzymatic concentrations), isolated PP_2 yields oscillations over a range of G_2 concentration, albeit with different amplitude and period than PP_1. We have also modified G_2 with a fluorescent dye so that it produces a red signal reporting on the prey N_2 (Figure 4a and Supporting Information Figures S12 and S13).

When PP_2 is run in combination with PP_1, in the same tube, the four species N_1, P_1, N_2, and P_2 compete for the access to enzymatic resources. Experimentally, we observe radical changes of the individual trajectories (Figure 4 and Supporting Information Figures S14−S18). In a closed system, permanent regimes are by definition impossible, and only transient responses can be observed, impeding the classification of the observed behaviors into general dynamic categories. Hints of period doubling, synchronization, and chaotic behavior (with sensitivity to initial conditions, Figure 4f and Supporting Information movie S3) can, however, be gathered from the experimental time courses at various G_1/G_2 concentration ratios.

These behaviors can be qualitatively understood by considering two conflicting influences: on the one hand, each PP pair has its own characteristic period, controlled solely by the concentration of its G template. On the other hand, competitive inhibition of the various enzymatic reactions will intuitively tend to

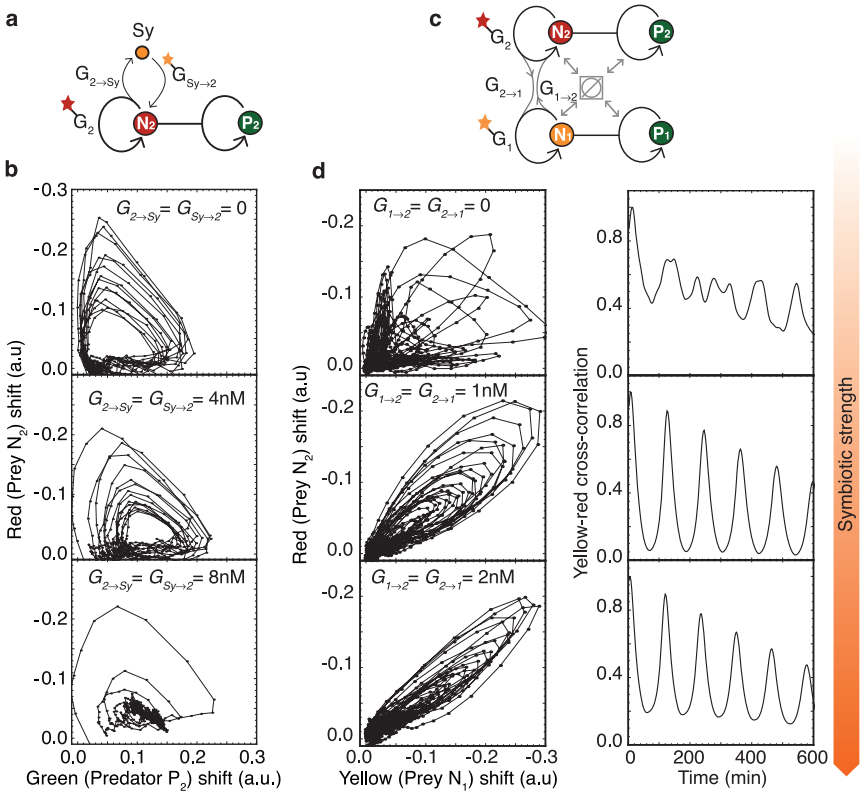

Figure 5. Effect of symbiosis on molecular PP systems. (a) Predator–prey–mutualist network. Template $G_{2\to sy}$ produces the symbiont Sy in the presence of N_2. Template $G_{Sy\to 2}$ does the opposite and is 3′-labeled with the yellow dye Dy530 to report on the presence of Sy (see Supporting Information Figure S22). The concentrations of these templates define the strength and symmetry of the symbiotic interaction. (b) Experimental trajectories with increasing (and symmetric) symbiosis between N_2 and Sy. The plots show the prey *versus* predator trajectories in the fluorescence space. Increasing the symbiotic link dampens the oscillations and allows the trajectory to settle quickly on a steady state (bottom plot). (c) Two PP pairs with global resource competition and bilateral symbiosis between the two preys. $G_{1\to 2}$ and $G_{2\to 1}$ control the strength of the symbiotic relation. (d) Red (N_2) *versus* yellow (N_1) trajectories (left column) and cross-correlations (right column) showing the synchronizing and phase locking effect of increased symbiosis.

synchronize the two systems: a given PP pair feels the current phase of the other pair through the changes in the apparent activity of the enzymatic resources and will thus experience a form of periodic forcing. In particular, the degradation step has the smallest saturation constant (Table S5). Therefore, in Figure 4g, competition for the exonuclease was used as the dominant interpair coupling force in a four-species mathematical model (Supporting Information Figures S19–S21). Depending on the concentration of templates G_1 and G_2, numerical solving predicts the alternation of synchronized zones (possibly with higher periodicity) and chaotic areas. Some of the computed trajectories (Figure 4h) bear a strong resemblance with the experimental ones, notwithstanding the expected sensitivity to the parameter values.

Symbiosis is the third type of fundamental interaction that shapes the dynamics of ecosystems. A mutualistic species (*i.e.* having a reciprocally beneficial relationship with another species) can combine with predator–prey interactions in a variety of manners and with diverse dynamic outcomes.[26,27] In the case of two predator–prey pairs, it was predicted that weak mutualism at the prey level would generate in-phase synchronization of the two oscillators.[28]

In Figure 5, we endow the previous chemical models with two kinds of symbiotic interactions. First, we focus on the single PP_2 pair with a mutualistic interaction between the prey P_2 and a third species, Sy, that is, a predator–prey–mutualist system.[26] We do this by including two cross-catalytic templates $G_{2\to Sy}$ and $G_{Sy\to 2}$ in the mix, along with the autocatalytic G_2 (Figure 5a). $G_{2\to Sy}$ works in the same way as G_2 (Figure 1), except that it produces Sy instead of a second copy of N_2. $G_{Sy\to 2}$ does the contrary. The presence of these two templates enforces that the mutualist Sy is created from N_2 and, in turn, fosters the growth of N_2. We observe that, as the mutualistic interaction increases in strength (*i.e.*, the templates $G_{2\to Sy}$ and $G_{Sy\to 2}$ increase in concentration), the sustained oscillations that were initially observed get damped and are replaced by the stable coexistence of all three species (Figure 5b). In a second set of experiments, mutualism is enforced between the two prey of the two pairs PP_1 and PP_2. To do this, we add the templates $G_{1\to 2}$ and $G_{2\to 1}$, in equal concentration, to the G_1/G_2 mix, therefore

embedding cross-catalysis at the prey level (Figure 5c). In line with theoretical predictions,[28] we now observe the gradual synchronization and in-phase locking of the two oscillators (Figure 5d, Supporting Information Figures S22 and S23 for simulations).

Discussion. With its predictable secondary structures and rich biochemistry, DNA provides a flexible substrate for the building of reaction networks with tailored topologies.[16] The batch assembly of out-of-equilibrium dynamics further requires the design of a reliable internal energy source as well as an efficient chemical sink. This was addressed here by the use of enzymatic catalysis. We have thus shown that, by combining DNA versatility and enzymatic tools, concepts such as predation or symbiosis, usually associated with living ecosystems, may be given a chemical implementation.[29] It is striking that many of the exotic dynamics observed or predicted for real animal populations[4−6,25,26,30,31] can be reproduced in our abiotic molecular setup. Important ecological questions such as the behavior of spatially distributed PP systems,[14,32] the role of stochastic effects when population size goes down to a few individuals,[33] and the coupling with environmental cycles[5] will now become open to *in vitro* investigation with chemical models. We also envision the use of such molecular tools to explore the relation between stability and complexity in ecosystems[34] or the interplay with evolutionary dynamics.[35,36]

From a practical point of view, the molecular programming strategy reported here is extremely compact—the PP system is fully encoded on a single 20 base template—and yields very robust behaviors. Together with the Belousov−Zhabotinsky and a handful of other reactions, it is one of the few schemes that are able to display tens of oscillations in a closed setting.[9,16] Contrary to small-molecule oscillators, however, our approach is general in the sense that many systems with various reaction network topologies can be built using the same design principles. Another important asset of DNA-based systems is that they can be interfaced with other downstream or upstream modules,[37] as we have shown here with the symbiotic networks. Therefore, beside opening the way to the study of fundamental issues of chemical dynamic systems, we also expect that this approach will provide a useful building block in the scaling-up of molecular computers[12,38] and machines.[39,40]

METHODS

Sequence Design. Designing PP systems comes down to selecting the sequence of the G template, which solely controls the structure of the reaction network. This sequence is a dual repeat including the following features: the recognition site of a nicking enzyme with the nicking position between the two repeats of the complementary strand (*i.e.*, between the two prey); the absence of this recognition site anywhere else in the system; and the partially palindromic sequence of each repeat (allowing prey extension into predators that are fully palindromic, while short). The template should also be resistant to exonuclease degradation, which can be achieved with a few phosphorothioate backbone modifications at the 5′ end.[16]

Reaction Assembly and Monitoring. Throughout the study, we have used a buffer containing 20 mM Tris-HCl, 10 mM $(NH_4)_2SO_4$, 10 mM KCl, 50 mM NaCl, 8 mM $MgSO_4$, 400 μM each dNTP (NEB), 0.1% Synperonic F108 (Aldrich), 5 ng/μL extremely thermostable single-strand binding protein (ETSSB; NEB), 100 μg/mL BSA (NEB), 2 μM Netropsin (Sigma Aldrich), 4 mM DTT, 1× EvaGreen (Biotium), 0.5× ROX (from a standard 100× dilution provided by Invitrogen), and a pH of 8.8. The function of each component of the buffer is detailed in Supporting Information Methods section. All experiments (except otherwise specified) were performed at T = 46.5 °C, with 3.7 nM Bst, 600 units/mL Nb.BsmI, 32.5 nM ttRecJ. Reactions were typically run in parallel in strips of 20 μL PCR white tubes, with various concentrations of templates G and initiated with a small amount of the corresponding prey and predators. After assembly of all of the components, the tubes were carefully vortexed, centrifuged, and transferred in a Bio-Rad CFX or MiniOpticon thermocycler set at a constant temperature. The fluorescence records were obtained from the real-time thermocyclers at intervals of a few minutes (for the oscillating experiments). The fluorescence cross-talks between the different channels (green, yellow, and deep red) were removed by the built-in software after calibration for EvaGreen (ex. 500 nm, em. 530 nm), Dy530 (ex. 539 nm, em. 561 nm), JOE (ex. 520, em. 548), and Dy681 (ex. 691 nm, em. 708 nm). Before analysis, these crude data sets were detrended to eliminate the background fluorescence and long-term drifts.

Simulations. The two-variable model was derived from the mechanistic description under the approximation of small binding constants for hybridization reactions. An initial set of parameters was obtained by kinetic analysis of the individual reactions as described in Supporting Information section 3 and latter refined by direct fitting of the experimental oscillating traces (using Mathematica). Bifurcation diagrams were built either by analytical stability analysis of the fixed points of the models (for the simple case of a single PP pair) or by numerical integration of the time series (in more complex cases).

Conflict of Interest: The authors declare no competing financial interest.

Acknowledgment. We thank A. Padirac, A. Genot, and H. Guillou for comments on the manuscript. We also thank K. Tabata and A. Yamagata for advice, and R. Masui for a gift of the thermophilic exonuclease. This work was supported by the CNRS and a Grant-in-Aid for Scientific Research on Innovative Areas from MEXT, Japan.

Supporting Information Available: Additional figures and experimental details as described in text. This material is available free of charge *via* the Internet at http://pubs.acs.org.

REFERENCES AND NOTES

1. Lotka, A. Undamped Oscillations Derived from the Law of Mass Action. *J. Am. Chem. Soc.* **1920**, *42*, 1595–1599.
2. Volterra, V. Fluctuations in the Abundance of a Species Considered Mathematically. *Nature* **1926**, *118*, 558–560.
3. Turchin, P. *Complex Population Dynamics: A Theoretical/Empirical Synthesis*; Princeton University Press: Princeton, NJ, 2003.
4. Huffaker, C. Experimental Studies on Predation: Dispersion Factors and Predator−Prey Oscillations. *Hilgardia* **1958**, *27*, 343–383.
5. Grover, J.; Mckee, D.; Young, S.; Godfray, H.; Turchin, P. Periodic Dynamics in Daphnia Populations: Biological Interactions and External Forcing. *Ecology* **2000**, *81*, 2781–2798.

6. Benincà, E.; Huisman, J.; Heerkloss, R.; Jöhnk, K. D.; Branco, P.; Van Nes, E. H.; Scheffer, M.; Ellner, S. P. Chaos in a Long-Term Experiment with a Plankton Community. *Nature* **2008**, *451*, 822–825.
7. Goodwin, R. M. *Essays in Economic Dynamics*; MacMillan Press Ltd.: United Kingdom, 1982.
8. Hodrick, R. J.; Prescott, E. C. Postwar US Business Cycles: An Empirical Investigation. *Journal of Money, Credit and Banking* **1997**, 1–16.
9. Epstein, I. R.; Pojman, J. A. *An Introduction to Nonlinear Chemical Dynamics*; Oxford University Press: New York, 1998.
10. Ackermann, J.; Wlotzka, B.; McCaskill, J. S. *In Vitro* DNA-Based Predator–Prey System with Oscillatory Kinetics. *Bull. Math. Biol.* **1998**, *60*, 329–354.
11. Wlotzka, B.; McCaskill, J. S. A Molecular Predator and Its Prey: Coupled Isothermal Amplification of Nucleic Acids. *Chem. Biol.* **1997**, *4*, 25–33.
12. Soloveichik, D.; Seelig, G.; Winfree, E. DNA as a Universal Substrate for Chemical Kinetics. *Proc. Natl. Acad. Sci. U.S.A.* **2010**, *107*, 5393–5398.
13. Lotka, A. Contribution to the Theory of Periodic Reactions. *J. Phys. Chem.* **1910**, *14*, 271–274.
14. Boerlijst, M. C.; Hogeweg, P. Spiral Wave Structure in Pre-Biotic Evolution: Hypercycles Stable Against Parasites. *Phys. D* **1991**, *48*, 17–28.
15. Schuster, P.; Sigmund, K. Replicator Dynamics. *J. Theor. Biol.* **1983**, *100*, 533–538.
16. Montagne, K.; Plasson, R.; Sakai, Y.; Fujii, T.; Rondelez, Y. Programming an *In Vitro* DNA Oscillator Using a Molecular Networking Strategy. *Mol. Syst. Biol.* **2011**, *7*, 466.
17. Kim, J.; Winfree, E. Synthetic *In Vitro* Transcriptional Oscillators. *Mol. Syst. Biol.* **2011**, *7*, 465.
18. Padirac, A.; Fujii, T.; Rondelez, Y. Bottom-Up Construction of *In Vitro* Switchable Memories. *Proc. Natl. Acad. Sci. U.S.A.* **2012**, *109* (47), E3212–E3220.
19. Genot, A. J.; Fujii, T.; Rondelez, Y. Computing with Competition in Biochemical Networks. *Phys. Rev. Lett.* **2012**, *109*, 208102.
20. Rondelez, Y. Competition for Catalytic Resources Alters Biological Network Dynamics. *Phys. Rev. Lett.* **2012**, *108*, 018102.
21. Lincoln, T. A.; Joyce, G. F. Self-Sustained Replication of an RNA Enzyme. *Science* **2009**, *323*, 1229–1232.
22. Li, T.; Nicolaou, K. C. Chemical Self-Replication of Palindromic Duplex DNA. *Nature* **1994**, *369*, 218–221.
23. Wakamatsu, T.; Kitamura, Y.; Kotera, Y.; Nakagawa, N.; Kuramitsu, S.; Masui, R. Structure of RecJ Exonuclease Defines Its Specificity for Single-Stranded DNA. *J. Biol. Chem.* **2010**, *285*, 9762–9769.
24. Padirac, A.; Fujii, T.; Rondelez, Y. Quencher-Free Multiplexed Monitoring of DNA Reaction Circuits. *Nucleic Acids Res.* **2012**, *40*, e118.
25. Vandermeer, J. Loose Coupling of Predator–Prey Cycles: Entrainment, Chaos, and Intermittency in the Classic Macarthur Consumer-Resource Equations. *Am. Nat.* **1993**, *141*, 687–716.
26. Rai, B.; Freedman, H. I.; Addicott, J. F. Analysis of Three Species Models of Mutualism in Predator–Prey and Competitive Systems. *Math. Biosci.* **1983**, *65*, 13–50.
27. Kooi, B. W.; Kuijper, L. D. J.; Kooijman, S. A. L. M. Consequences of Symbiosis for Food Web Dynamics. *J. Math. Biol.* **2004**, *49*, 227–271.
28. Vandermeer, J. Coupled Oscillations in Food Webs: Balancing Competition and Mutualism in Simple Ecological Models. *Am. Nat.* **2004**, *163*, 857–867.
29. Lemarchand, A.; Jullien, L. Competition and Symbiosis in a Chemical World. *J. Phys. Chem. B* **2004**, *108*, 11782–11791.
30. May, R. Limit Cycles in Predator–Prey Communities. *Science* **1972**, *177*, 900.
31. Hastings, A.; Powell, T. Chaos in a Three-Species Food Chain. *Ecology* **1991**, *72*, 896–903.
32. Gurney, W.; Veitch, A.; Cruickshank, I.; McGeachin, G. Circles and Spirals: Population Persistence in a Spatially Explicit Predator–Prey Model. *Ecology* **1998**, *79*, 2516–2530.
33. Mckane, A. J.; Newman, T. J. Predator–Prey Cycles from Resonant Amplification of Demographic Stochasticity. *Phys. Rev. Lett.* **2005**, *94*, 218102.
34. Allesina, S.; Tang, S. Stability Criteria for Complex Ecosystems. *Nature* **2012**, *483*, 205–208.
35. Johns, G. C.; Joyce, G. F. The Promise and Peril of Continuous *In Vitro* Evolution. *J. Mol. Evol.* **2005**, *61*, 253–263.
36. Page, K. M.; Nowak, M. A. Unifying Evolutionary Dynamics. *J. Theor. Biol.* **2002**, *219*, 93–98.
37. Franco, E.; Friedrichs, E.; Kim, J.; Jungmann, R.; Murray, R.; Winfree, E.; Simmel, F. C. Timing Molecular Motion and Production with a Synthetic Transcriptional Clock. *Proc. Natl. Acad. Sci. U.S.A.* **2011**, *108*, E784–93.
38. Qian, L.; Winfree, E. Scaling up Digital Circuit Computation with DNA Strand Displacement Cascades. *Science* **2011**, *332*, 1196–1201.
39. Douglas, S. M.; Bachelet, I.; Church, G. M. A Logic-Gated Nanorobot for Targeted Transport of Molecular Payloads. *Science* **2012**, *335*, 831–834.
40. Wickham, S. F. J.; Bath, J.; Katsuda, Y.; Endo, M.; Hidaka, K.; Sugiyama, H.; Turberfield, A. J. A DNA-Based Molecular Motor That Can Navigate a Network of Tracks. *Nat. Nanotechnol.* **2012**, *7*, 169–173.